Ensemble quantum-information processing by NMR: Implementation of gates and the creation of pseudopure states using dipolar coupled spins as qubits

T. S. Mahesh,[1] Neeraj Sinha,[1] K. V. Ramanathan,[2] and Anil Kumar[1,2,*]
[1]*Department of Physics, Indian Institute of Science, Bangalore 560012, India*
[2]*Sophisticated Instruments Facility, Indian Institute of Science, Bangalore 560012, India*
(Received 12 August 2001; published 11 January 2002)

Quantum-information processing is carried out using dipolar coupled spins and high-resolution nuclear magnetic resonance (NMR). The systems chosen are the dipolar coupled methyl protons of CH_3CN partially oriented in a liquid crystalline matrix yielding a two-qubit system and dipolar coupled ^{13}C and methyl protons of $^{13}CH_3CN$ also partially oriented in the liquid crystalline matrix, yielding a three-qubit system. The dipolar coupled protons of oriented CH_3 group are chemically and magnetically identical and their eigenstates can be divided into a set of quartet states (symmetric A) and a pair of doublet (E) states. We describe here a method for selectively retaining the magnetization of the symmetric states, yielding two and three qubit systems. We create pseudopure states using single-quantum-transition selective pulses and implement two- and three-qubit gates using one- and two-dimensional NMR.

DOI: 10.1103/PhysRevA.65.022312 PACS number(s): 03.67.−a

I. INTRODUCTION

The field of quantum-information processing involving quantum computation, cryptography, error correction, and teleportation has shown an exponential growth during recent years. Several quantum algorithms have been developed and the advantages of quantum-information processing have been clearly established. Many experimental methods have been suggested, out of which liquid-state nuclear magnetic resonance (NMR) has shown the largest progress towards quantum-information processing. Pseudopure states [1–10], logic gates [4,11–15], the Deutch-Jozsa algorithm [5,16–19], Grover's search algorithm [20,21], and the quantum Fourier transform [22] have been implemented by liquid-state NMR. One of the limitations of liquid-state NMR is the difficulty in scaling up the number of qubits available for quantum computing [23]. Most of the NMR quantum computing so far has utilized systems having indirect spin-spin coupling (also known as J coupling) [4,18,21–25]. These couplings are mediated via the covalent bonds and are vanishingly small for more than four bonds. This restricts the number of qubits one can have in J-coupled NMR. A more attractive coupling for information processing is the direct dipolar coupling between the spins, which has larger magnitude and range and does not require covalent bonds. In liquids the dipolar couplings are averaged to zero due to rapid isotropic reorientations of the molecules and in rigid solids there are too many couplings, yielding broad lines. In molecules partially oriented in anisotropic media, such as liquid crystals, one obtains a finite number of dipolar coupled spins. Such systems thus provide suitable candidates for quantum-information processing and so far have been utilized for creation of pseudopure states, implementation of a controlled-NOT (C-NOT) gate, application of Grover's search algorithm, and for creation of Einstein-Podolsky-Rosen states [26–28]. Attempts are also being made to utilize spins with $I>\frac{1}{2}$ (mainly $\frac{3}{2}$ and $\frac{7}{2}$ spins as two- and three-qubit systems) oriented in liquid-crystalline matrices having quadrupolar couplings [29–32].

In this paper we utilize oriented methyl groups to form two- and three-qubit systems. While the feasibility of using the oriented methyl group for quantum-information processing has been demonstrated earlier [28], we have added several features to this system. First, we describe a method for selectively retaining the magnetization of the symmetric eigenstates of the oriented methyl protons. This is an important improvement over the earlier experiments, which described only the creation of pseudopure states without removing the degenerate doublet transitions [28]. Second, we create pseudopure states using the recently proposed spatially averaged logical-labeling technique (SALLT) [10], and finally, we utilize transition selective pulses to implement a number of two- and three-qubit logic gates.

II. THE ORIENTED CH_3 GROUP

The NMR Hamiltonian for an oriented molecule is given by [33,34]

$$\mathcal{H}=\sum_i \omega_i I_z^i+\sum_{i<j}(J_{ij}+2D_{ij})I_z^iI_z^j + \tfrac{1}{2}\sum_{i<j}(J_{ij}-D_{ij})(I_+^iI_-^j+I_-^iI_+^j), \quad (1)$$

where ω_i is the Larmor frequency and, J_{ij} and D_{ij} are, respectively, J couplings and residual dipolar couplings.

The eigenstates of this Hamiltonian for an A_3 spin system such as the protons of the CH_3 group fall into three manifolds [35] [Fig. 1(a)]: The quartet symmetric states (A) are

*Author to whom correspondence should be addressed. Email address: anilnmr@physics.iisc.ernet.in

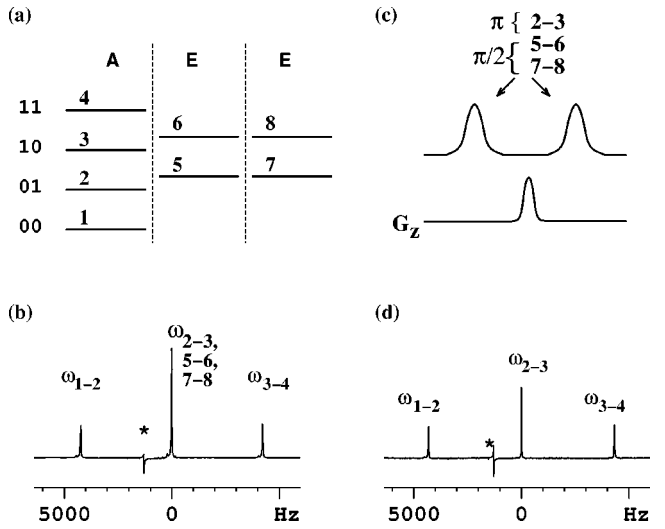

FIG. 1. (a) Energy-level diagram showing quartet (A) and doublet (E) manifolds of the oriented CH_3CN system and the two-qubit labeling scheme of the A manifold, (b) the equilibrium ^1H spectrum, (c) pulse sequence for selection of symmetric states (SOSS), and (d) the spectrum after SOSS. In (c), the transition-selective rf pulse on the central transition was of Gaussian shape and length 1 ms. The gradient pulse (G_z) was of strength 20 G/cm and length 1 ms. The integrated intensities of the peaks in (b) are in the ratio 3.1:6.1:3.0 (theoretically expected, 3:6:3). After SOSS, the integrated intensities are in the ratio 3.2:3.9:3.0 (theoretically expected, 3:4:3). The decrease in the intensity of the central transition corresponds to the saturation of the E manifolds. A small-angle nonselective detection pulse of length 1 μs was employed for linear measurement of populations in both (b) and (c). The small peak denoted by * is due to protons in the field-lock liquid and should be ignored.

$$|1\rangle = |+++\rangle,$$

$$|2\rangle = \frac{1}{\sqrt{3}}[|++-\rangle + |+-+\rangle + |-++\rangle],$$

$$|3\rangle = \frac{1}{\sqrt{3}}[|--+\rangle + |-+-\rangle + |+--\rangle],$$

$$|4\rangle = |---\rangle,$$

and the doublet states (E) are

$$|5\rangle = \frac{1}{\sqrt{3}}[|++-\rangle + \epsilon|+-+\rangle + \epsilon^2|-++\rangle],$$

$$|6\rangle = \frac{1}{\sqrt{3}}[|--+\rangle + \epsilon|-+-\rangle + \epsilon^2|+--\rangle],$$

$$|7\rangle = \frac{1}{\sqrt{3}}[|++-\rangle + \epsilon^2|+-+\rangle + \epsilon|-++\rangle],$$

$$|8\rangle = \frac{1}{\sqrt{3}}[|--+\rangle + \epsilon^2|-+-\rangle + \epsilon|+--\rangle],$$

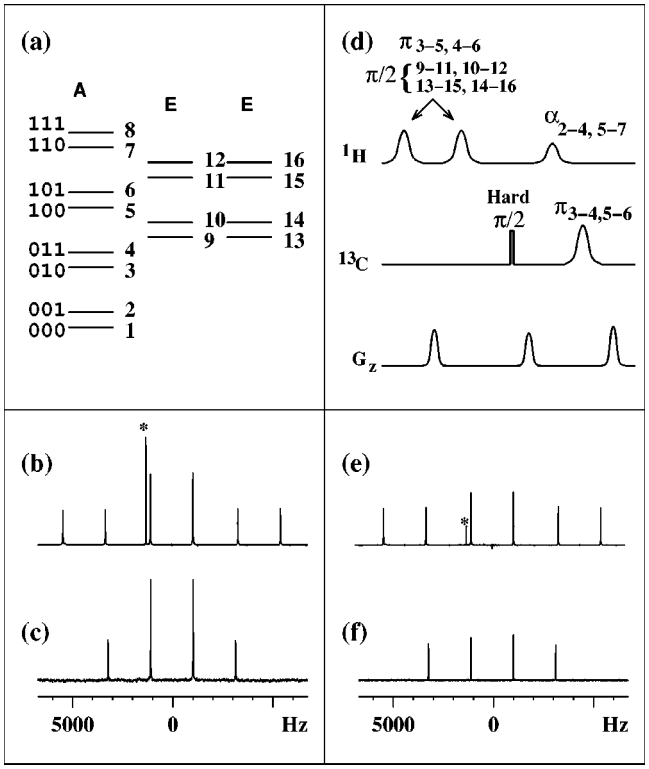

FIG. 2. (a) Energy-level diagram showing quartet (A) and doublet (E) manifolds of the oriented $^{13}CH_3CN$ system and the three-qubit labeling scheme of the A manifold. (b) The equilibrium ^1H and (c) ^{13}C spectra, (d) the scheme for selection of symmetric states (SOSS), (e) proton spectrum and (f) carbon spectrum after SOSS. The transition-selective rf pulses are of Gaussian shape and length 1 ms. The nonselective hard $\pi/2$ pulse on the ^{13}C was of rectangular shape and length 13 μs. The angle α of the transition-selective rf pulses on $1\leftrightarrow3$ and $6\leftrightarrow8$ for partial transfer of polarization to carbon was set to 30°. The sine-bell-shaped gradient pulses were of strength 20–30 G/cm and of length 1 ms. The experimental and theoretical (in parentheses) intensity ratios in equilibrium are 1.00:1.01:2.02:2.02:1.00:1.00 (1:1:2:2:1:1) in the ^1H spectrum and 1.17:3.02:2.85:1.00 (1:3:3:1) in the ^{13}C spectrum. The intensity ratios of various transitions of ^1H and ^{13}C after SOSS are $m{:}m{:}1{:}1{:}m{:}m{:}$ and 1:1:1:1, respectively, where $m = 3/[4(1 + 2\tan^2\alpha/2)]$. The experimental and the theoretical (in parentheses, for $\alpha = 30°$) ratios are 0.68:0.68:1.00:0.96:0.72:0.73 (0.66:0.66:1:1:0.66:0.66) in ^1H 1.00:1.00:1.04:0.95 (1:1:1:1) in ^{13}C spectra. All ^1H spectra were obtained with a nonselective small-angle detection pulse of length 1 μs. All ^{13}C spectra were obtained with a nonselective hard $\pi/2$ detection pulse of length 13 μs. The peaks marked by * are due to protons in the field-lock liquid and should be ignored.

where $\epsilon = e^{2\pi i/3}$, and + and − refer, respectively, to $+\frac{1}{2}$ and $-\frac{1}{2}$ states of each of the three protons.

Here states $|1\rangle$, $|2\rangle$, $|3\rangle$, and $|4\rangle$ form a symmetric (A) manifold yielding three single quantum transitions with frequencies $\omega_0 - 3D$, ω_0, and $\omega_0 + 3D$, where D is the residual dipolar coupling between the protons of the CH_3 group and ω_0 is their Larmor frequency. Transitions between the doublet states, namely, $|5\rangle\leftrightarrow|6\rangle$ and $|7\rangle\leftrightarrow|8\rangle$ also have the frequency of the central transition, ω_0. The resultant spectrum

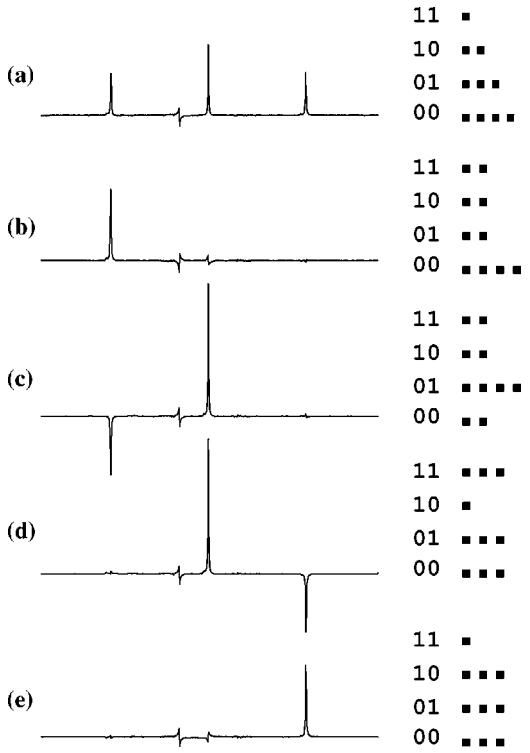

FIG. 3. (a) The equilibrium ^{1}H spectrum of oriented CH_3CN after SOSS, and spectra corresponding to different pseudopure states (b) $|00\rangle$, (c) $|01\rangle$, (d) $|10\rangle$, and (e) $|11\rangle$. The states and representative relative deviation populations are given on the right-hand side. The pseudopure states are prepared by using the spatial-averaging technique. The pulse sequences for preparing pseudopure states are as follows: (b) $\pi(10\leftrightarrow 11)-\pi/2(01\leftrightarrow 10)$ G, (c) state of (b) followed by $\pi(00\leftrightarrow 01)$ G, (d) state of (e) followed by $\pi(11\leftrightarrow 10)$ G, and (e) $\pi(01\leftrightarrow 10)-\pi/2(00\leftrightarrow 01)$ G. The rf pulses were of Gaussian shape and of length 1 ms. A gradient pulse (G) of strength 20 G/cm and length 1 ms was used to destroy all the coherence at the end of each pulse sequence before detection. All the spectra were obtained by a final nonselective small-angle detection pulse of length 1 μs corresponding to a flip angle of 10°. All the pseudopure states are prepared after implementing SOSS. The ratio of experimental and theoretical (in parentheses) intensities are (b) -0.02:-0.01:1 (0:0:1), (c) 0.05:1.33:-0.80 (0:1.33:-1), (d) -0.80:1.33:-0.03 (-1:1.33:0), and (e) 1.00:-0.05:-0.05 (1:0:0).

is a 3:6:3 triplet as shown in Fig. 1(b). Since intermanifold transitions are not allowed, the quartet manifold of this system, consisting of four energy levels, can be treated as a two-qubit system as shown in Fig. 1(a) [28]. The doublet manifolds can also be treated as a one-qubit system [8]. However, in the present case, we wish to use the symmetric (A) manifold of this system consisting of four energy levels as a two-qubit system. The E manifolds, which contribute to the central line, complicate the interpretation of results of logical operations. Therefore it is highly desirable to selectively saturate the E manifolds.

III. SELECTION OF SYMMETRIC STATES

Selection of symmetric states (SOSS) can be achieved by the selective saturation of the magnetization of doublet states

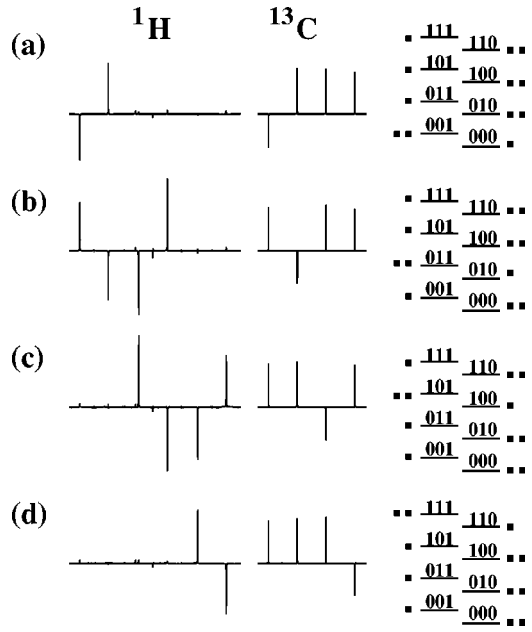

FIG. 4. ^{1}H (left) and ^{13}C (right) spectra corresponding to different subsystem pseudopure states (a) $|00\rangle$, (b) $|01\rangle$, (c) $|10\rangle$, and (c) $|11\rangle$ obtained by using SALLT [10]. Relative deviation populations of the two subsystems (corresponding to the states $|1\rangle$ and $|0\rangle$ of ^{13}C spin) are shown on the right-hand side. After implementing SOSS using the pulse sequence given in Fig. 2(d) with $\alpha=180°$, a nonselective $\pi/2$ pulse is applied on ^{1}H transitions. Then a transition-selective π pulse on one of the transitions of ^{13}C is applied, followed by a gradient pulse, yielding subsystem pseudopure states. The inverted ^{13}C transition can be identified from the ^{13}C spectrum. The ^{1}H and ^{13}C nonselective $\pi/2$ pulses were of rectangular shape and 9 μs in length. The transition selective ^{1}H and ^{13}C π pulses were of Gaussian shape and 4 ms length. The gradient pulses were of strength 20–30 G/cm and length 1 ms. All ^{1}H spectra were obtained by a final nonselective small-angle detection pulse of length 1 μs and all ^{13}C spectra were obtained by a nonselective $\pi/2$ detection pulse of length 13 μs. The ratio of experimental and theoretical (in parentheses) intensities of ^{1}H and ^{13}C spectra are (a) -1.00:1.12:0.05:0.06:0.01:0.03 (-1:1:0:0:0:0) and -0.74:1.06:1.05:1.00 (-1:1:1:1), (b) 1.00:-0.92:-1.27:1.37:0.04:0.07 (1:-1:-1.33:1.33:0:0) and 1.04:-0.72:1.10:1.00 (1:-1:1:1), (c) 0.06:0.02:1.33:-1.21:-0.85:1.00 (0:0:1.33:-1.33:-1:1) and 1.00:1.02:-0.72:1.10 (1:1:-1:1), and (d) 0.07:0.00:0.05:0.03:1.17:-1 (0:0:0:0:1:-1) and 1.00:1.05:1.08:-0.70 (1:1:1:-1).

by utilizing the fact that the nutation frequency for the transition $2\leftrightarrow 3$ is double the nutation frequencies of $5\leftrightarrow 6$ and $7\leftrightarrow 8$ [35], since

$$|\langle 2|I_x|3\rangle| = 2|\langle 5|I_x|6\rangle| = 2|\langle 7|I_x|8\rangle|. \tag{2}$$

Therefore, a selective π pulse on transition $2\leftrightarrow 3$ acts simultaneously as a $\pi/2$ pulse on transitions $5\leftrightarrow 6$ and $7\leftrightarrow 8$. The pulse sequence for SOSS is given in Fig. 1(c). A single rf pulse on the central transition inverts the populations of $|2\rangle$ and $|3\rangle$ and equalizes the populations of $|5\rangle$ and $|6\rangle$, and $|7\rangle$ and $|8\rangle$. A subsequent gradient pulse destroys the transverse magnetization of the E manifolds created by the $\pi/2$ pulse,

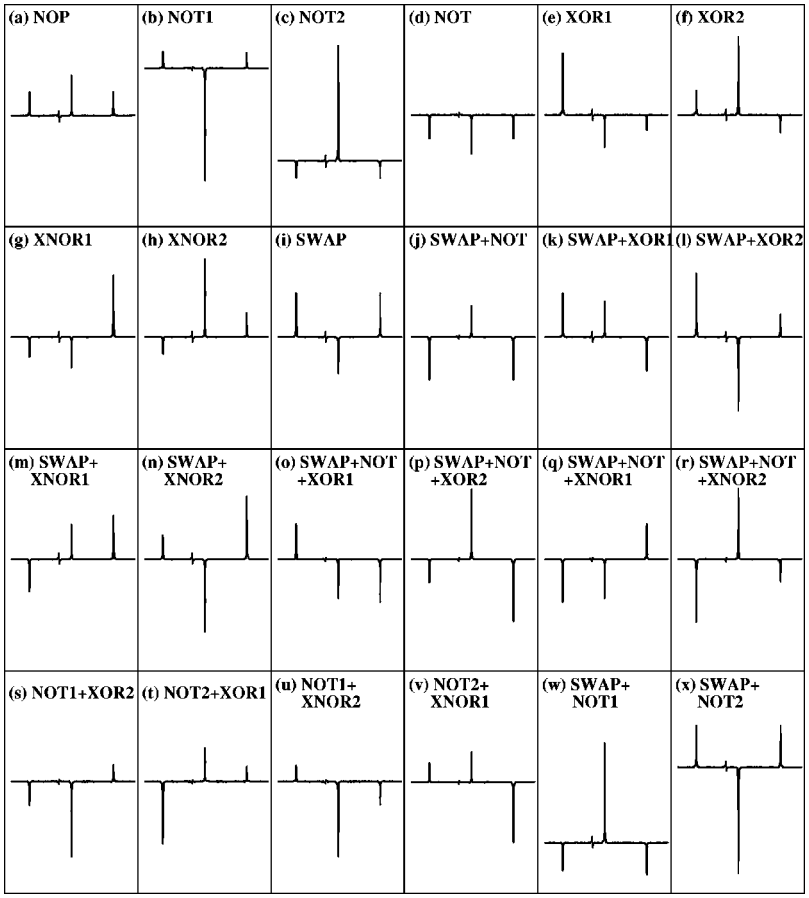

FIG. 5. ^{1}H spectra of oriented CH_3CN corresponding to a complete set of two-qubit one-to-one gates implemented (after applying SOSS) using transition-selective rf pulses. The unitary operator and pulse sequence corresponding to each gate are given in [30]. The nonselective π pulse was of rectangular shape and 9 μs in length while the transition-selective π pulse was of Gaussian shape and 1 ms length. All the spectra were obtained by a final nonselective small-angle detection pulse of length 1 μs.

thus saturating the doublet manifolds. The equilibrium populations of the symmetric A manifold can be restored by another π pulse on the $2\leftrightarrow3$ transition. Population distributions before and after SOSS are measured by applying a small-angle detection pulse. The resulting spectra are shown in Figs. 1(b) and 1(d), respectively. The spectrum after SOSS [Fig. 1(d)] from the symmetric A manifold is the expected 3:4:3 triplet.

A three-qubit system can be obtained by using a ^{13}C labeled acetonitrile ($^{13}CH_3CN$) oriented in a liquid crystal. Splitting of each energy level by the C-H coupling results in eight states for the A manifold and four states for each of the E manifolds [Fig. 2(a)]. The equilibrium ^{1}H and ^{13}C spectra of this system (before SOSS) are shown in Figs. 2(b) and 2(c), respectively. The SOSS pulse scheme for this system is shown in Fig. 2(d). To saturate all the transitions of the E manifolds, one has to carry out SOSS separately in both proton and carbon transitions. SOSS in protons can be carried out as follows. A selective π pulse in transitions $|3\rangle\leftrightarrow|5\rangle$ and $|4\rangle\leftrightarrow|6\rangle$ inverts the populations of the A states, but acts as a $\pi/2$ pulse on E transitions $|9\rangle\leftrightarrow|11\rangle$, $|10\rangle\leftrightarrow|12\rangle$, $|13\rangle\leftrightarrow|15\rangle$, and $|14\rangle\leftrightarrow|16\rangle$, equalizing their populations. A subsequent gradient pulse destroys the coherence of E states created by the $\pi/2$ pulse. Another selective π pulse on transitions $|3\rangle\leftrightarrow|5\rangle$ and $|4\rangle\leftrightarrow|6\rangle$ restores the equilibrium populations of A states. To saturate all the E states, we also need to implement SOSS on ^{13}C E states. However, nutation frequencies of ^{13}C transitions are same in A and E manifolds. To achieve SOSS in ^{13}C the following procedure has been adopted. After the SOSS in protons, a nonselective $\pi/2$ pulse on ^{13}C followed by a gradient pulse saturates all the ^{13}C states. However, to treat the eight eigenstates of the A manifold as a three-qubit system, carbon polarization of A states is required. This is achieved by a partial polarization transfer from A transitions of ^{1}H to the A transitions of ^{13}C, by applying a selective α pulse on ^{1}H transitions $|2\rangle\leftrightarrow|4\rangle$ and $|5\rangle\leftrightarrow|7\rangle$, followed by selective π pulses on ^{13}C transitons $|3\rangle\leftrightarrow|4\rangle$ and $|5\rangle\leftrightarrow|6\rangle$. The angle α of the pulse decides the amount of proton polarization transferred to the carbon and can be chosen depending on the desired initial state. A final gradient pulse destroys all the transverse magnetization generated during the process. The ^{1}H and ^{13}C spectra after complete SOSS are given in Figs. 2(e) and 2(f), respectively. After saturating all the E states, the system can be treated as a three-qubit system.

IV. PREPARATION OF PSEUDOPURE STATES

Implementation of quantum algorithms generally begins with definite input states [36]. Since NMR is an ensemble technique, preparation of such definite input states called ''pure states'' is difficult and therefore this problem is circumvented by the preparation of ''effective pure states'' or ''pseudopure states,'' which mimic pure states. Many methods have been proposed for preparing pseudopure states in NMR [1–8,10,28]. In the present two-qubit system pseudopure states are prepared by spatial averaging method [1,4,30] as shown in Fig. 3. For example, the $|00\rangle$

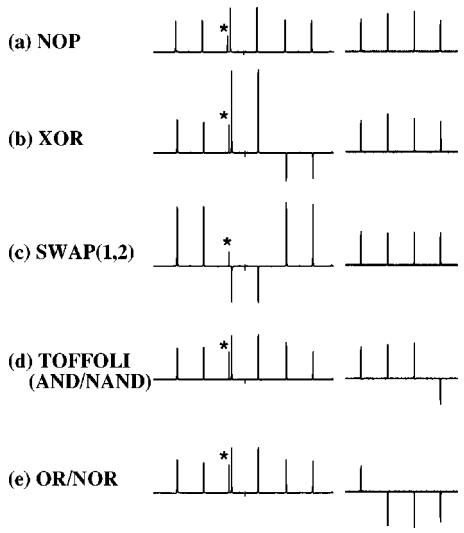

FIG. 6. ^{1}H (left) and ^{13}C (right) spectra of oriented $^{13}CH_3CN$ corresponding to various three-qubit gates implemented using spin- and transition-selective pulses. All gates are implemented after implementing SOSS. The pulse sequences for the above gates are as follows [see Fig. 2(a) for state labels]. (a) No operation gate (NOP) no computation pulse; (b) XOR2 gate ($|x,y,z\rangle \rightarrow |x,x,\oplus y,z\rangle$), $\pi(100\leftrightarrow 110,101\leftrightarrow 111)$; (c) SWAP (1,2) gate, $\pi(100\leftrightarrow 010, 101\leftrightarrow 011)$; (d) Toffoli gate ($C^2$-NOT), $\pi(110\leftrightarrow 111)$; (e) OR/NOR gate, π (nonselective on ^{13}C,) $\pi(000\leftrightarrow 001)$. The nonselective pulse on ^{13}C was of rectangular shape and length 13 μs. The transition-selective pulses were of Gaussian shape and 4 ms length. All ^{1}H spectra were obtained by a final nonselective small-angle detection pulse of length 1 μs. All ^{13}C spectra were obtained by a final nonselective rectangular $\pi/2$ pulse of length 13 μs. The peaks marked by * should be ignored.

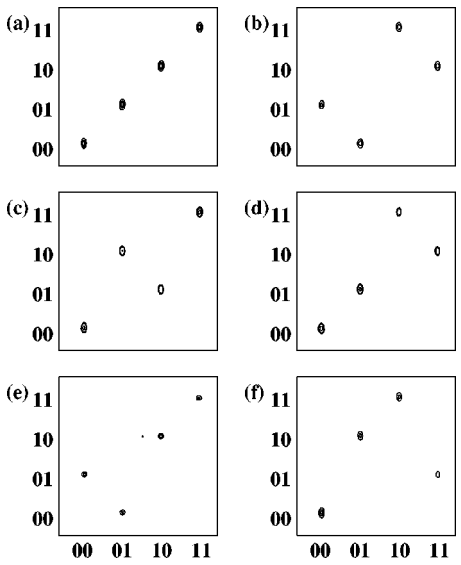

FIG. 7. ^{13}C spectra of oriented $^{13}CH_3CN$ corresponding to various two-qubit gates implemented using transition-selective pulses and two-dimensional NMR. All gates are implemented after SOSS on both ^{1}H and ^{13}C. The general pulse scheme for 2D gates is discussed in the text. The computation pulses for the above gates are as follows [see Fig. 2(a) for state labels]: (a) No operation gate NOP no computation pulse; (b) NOT2 gate, $\pi(000\leftrightarrow 010) - \pi(001\leftrightarrow 011) - \pi(100\leftrightarrow 110 - \pi(101\leftrightarrow 111)$; (c) SWAP gate, $\pi(010\leftrightarrow 100) - \pi(011\leftrightarrow 101)$; (d) XOR2 gate, $\pi(110\leftrightarrow 100) - \pi(111\leftrightarrow 101)$; (e) XNOR2 gate, $\pi(000\leftrightarrow 010) - \pi(001\leftrightarrow 011)$; (f) SWAP+XOR2 [combination of (c) and (e) pulse sequences]. The nonselective $\pi/2$ pulses on ^{13}C were of rectangular shape and 13 μs length while the transition-selective computation pulses on ^{1}H were of Gaussian shape and 4 ms length. All experiments were carried out in the time domain with $128t_1$ values and 128 complex data points along t_2. Zero filling to 512×512 complex data points was done prior to the 2D Fourier transformation.

pseudopure state has been created by a selective π pulse on $|10\rangle\leftrightarrow|11\rangle$ transition followed by a selective $\pi/2$ pulse on $|10\rangle\leftrightarrow|01\rangle$ transition and a gradient to destroy unwanted coherence. This will equalize the populations of all the states except $|00\rangle$ [Fig. 3(b)]. In each case the final population distribution is measured by a nonselective small-flip-angle ($\pi/10$) pulse. In the three-qubit system of $^{13}CH_3CN$ pseudopure states are prepared by using the recently proposed SALLT method [10]. In this method two subsystems can be identified corresponding to 0 and 1 spin states of ^{13}C. A hard $\pi/2$ pulse on ^{1}H equalizes the populations of all the ^{1}H states and a subsequent gradient destroys the coherence created by the $\pi/2$ pulse. This followed by a selective π pulse on one of the four transitions of ^{13}C yields a pair of subsystem pseudopure states, as shown in Fig. 4.

V. IMPLEMENTATION OF GATES

A. Using one-dimensional NMR

A complete set of two-qubit reversible logic gates on CH_3CN system has been implemented (after applying SOSS) using transition-selective pulses (Fig. 5). For example, NOT2 (index 2 indicates the position of the output qubit) requires a π pulse on all transitions followed by selective π pulses on $1\leftrightarrow 2$ and $3\leftrightarrow 4$ transitions (see Fig. 1 for labeling). NOT describes NOT operation on both qubits and is achieved by a single π pulse on all transitions. XNOR2 requires a selective π pulse on $1\leftrightarrow 2$ transition. The pulse sequence and the unitary operators for each of the 24 gates are discussed in [30]. Figure 6 contains several three-qubit gates implemented on the three-qubit system of $^{13}CH_3CN$ using one-dimensional NMR. All the two- and three-qubit gates have been implemented after the application of SOSS. The pulse sequences for each case are given in the caption of Fig. 6.

B. Using two-dimensional NMR

Utilizing two-dimensional (2D) NMR for implementing quantum logic gates has been demonstrated recently [12,14,37]. In this method, an extra qubit called ''observer qubit'' is used to label the transitions of ''input qubits.'' The observer qubit is allowed to evolve during t_1 period and then stored in Zeeman direction. A gradient pulse is applied to remove all transverse magnetization, which is followed by computation pulses on the input qubits. After the computation pulse, the observer qubit is again brought to the transverse direction and its free evolution is detected in time t_2. The resulting 2D spectrum gives a direct correlation between

input and output of a gate. In this case, ^{13}C spin is chosen as the observer qubit and the A manifold of ^{1}H spins correspond to the states of input qubits. NOT, NOT2, SWAP, XOR2, XNOR2, and SWAP+XOR2 gates have been implemented after SOSS (Fig. 7). It may be mentioned that, without SOSS one obtains two extra peaks on the diagonal in all the 2D gates, interfering with the interpretation of the gates. To the best of our knowledge this is the first implementation of logic gates on dipolar coupled spins using two-dimensional NMR.

VI. CONCLUSIONS

Dipolar couplings among oriented nuclear spins offer attractive possibilities for increasing the number of qubits in quantum-information processing by NMR. A beginning has been made by using the oriented methyl protons, which have been made to yield a two-qubit system. Coupling to heteronuclei offers many possibilities. One qubit has been added by using a labeled carbon-13. Attempts are underway to increase the number of qubits to four by using oriented $^{13}CH_3C^{15}N$.

ACKNOWLEDGMENT

The use of the 500-MHz FTNMR spectrometer of the Sophisticated Instruments Facility (SIF), Indian Institute of Science, funded by Department of Science and Technology, New Delhi is gratefully acknowledged.

[1] D. G. Cory, A. F. Fahmy, and T. F. Havel, Proc. Natl. Acad. Sci. U.S.A. **94**, 1634 (1997).
[2] N. Gershenfeld and I. L. Chuang, Science **275**, 350 (1997).
[3] E. Knill, I. L. Chuang, and R. Laflamme, Phys. Rev. A **57**, 3348 (1998).
[4] D. G. Cory, M. D. Price, and T. F. Havel, Physica D **120**, 82 (1998).
[5] Kavita Dorai, Arvind, and Anil Kumar, Phys. Rev. A **61**, 042306 (2000).
[6] U. Sakaguchi, H. Ozawa, and T. Fukumi, Phys. Rev. A **61**, 042313 (2000).
[7] Y. Sharf, T. F. Havel, and D. G. Cory, Phys. Rev. A **62**, 052314 (2000).
[8] E. Knill, R. Laflamme, R. Martinez, and C. H. Tseng, Nature (London) **404**, 368 (2000).
[9] X. Peng, X. Zhu, X. Fang, M. Feng, K. Gao, and M. Liu, e-print quant-ph/0012038.
[10] T. S. Mahesh and Anil Kumar, Phys. Rev. A **64**, 012307 (2001).
[11] J. A. Jones, R. H. Hansen, and M. Mosca, J. Magn. Reson. **135**, 353 (1998).
[12] Z. L. Madi, R. Bruschweiler, and R. R. Ernst, J. Chem. Phys. **109**, 10 603 (1998).
[13] J. A. Jones, Prog. Nucl. Magn. Reson. Spectrosc. **38**, 325 (2001).
[14] T. S. Mahesh, Kavita Dorai, Arvind, and Anil Kumar, J. Magn. Reson. **148**, 95 (2001).
[15] J. Du, M. Shi, J. Wu, X. Zhou, and R. Han, Phys. Rev. A **63**, 042302 (2001).
[16] D. Collins, K. W. Kim, W. C. Holton, H. Sierzputowska-Gracz, and E. O. Stejskal, Phys. Rev. A **62**, 022304 (2000).
[17] N. Linden, H. Barjat, and Ray Freeman, Chem. Phys. Lett. **296**, 61 (1998).
[18] J. A. Jones and M. Mosca, J. Chem. Phys. **109**, 1648 (1998).
[19] Arvind, Pramana **56**, 357 (2001).
[20] L. K. Grover, Phys. Rev. Lett. **79**, 325 (1997).
[21] I. L. Chuang, N. Gershenfeld, and M. Kubinec, Phys. Rev. Lett. **80**, 3408 (1998).
[22] Y. S. Weinstein, M. A. Pravia, E. M. Fortunato, S. Lloyd, and D. G. Cory, Phys. Rev. Lett. **86**, 1889 (2001).
[23] J. A. Jones e-print quant-ph/0002085.
[24] I. L. Chuang, N. Gershenfeld, M. G. Kubinec, and D. W. Leung, Proc. R. Soc. London, Ser. A **454**, 447 (1998).
[25] M. D. Price, S. S. Somaroo, A. E. Dunlop, T. F. Havel, and D. G. Cory, Phys. Rev. A **60**, 2777 (1999).
[26] C. S. Yannoni, M. H. Sherwood, D. C. Miller, I. L. Chuang, L. M. K. Vandersypen, and M. G. Kubinec, Appl. Phys. Lett. **75**, 3563 (1999).
[27] M. Marjanska, I. L. Chuang, and M. G. Kubinec, J. Chem. Phys. **112**, 5095 (2000).
[28] B. M. Fung, Phys. Rev. A **63**, 022304 (2001).
[29] A. K. Khitrin and B. M. Fung, J. Chem. Phys. **112**, 6963 (2000).
[30] Neeraj Sinha, T. S. Mahesh, K. V. Ramanathan, and Anil Kumar, J. Chem. Phys. **114**, 4415 (2001).
[31] A. Khitrin, H. Sun, and B. M. Fung, Phys. Rev. A **63**, 020301 (2001).
[32] K. V. R. M. Murali, Neeraj Sinha, T. S. Mahesh, K. V. Ramanathan, and Anil Kumar (unpublished).
[33] C. P. Slichter, *Principles of Magnetic Resonance* (Harper and Row, New York, 1978).
[34] P. Dhiel and C. L. Khetrapal, *NMR-Basic Principles and Progress* (Springer-Verlag, New York, 1996), Vol. 1, pp. 1–95.
[35] C. L. Mayne, J. M. Bernassau, and D. M. Grant, J. Chem. Phys. **76**, 257 (1982).
[36] J. Preskill, Lecture notes on quantum computation, http://theory.caltech.edu/people/preskill/ph229/
[37] Kavita Dorai, T. S. Mahesh, Arvind, and Anil Kumar, Curr. Sci. **79**, 1447 (2000).